UC Santa Cruz

UC Santa Cruz Previously Published Works

Title

Potent and Selective Inhibitors of Human Reticulocyte 12/15-Lipoxygenase as Anti-Stroke Therapies

Permalink

https://escholarship.org/uc/item/6697d2mz

Journal

Journal of Medicinal Chemistry, 57(10)

ISSN

0022-2623

Authors

Rai, Ganesha
Joshi, Netra
Jung, Joo Eun
et al.

Publication Date

2014-05-22

DOI

10.1021/jm401915r

# Potent and Selective Inhibitors of Human Reticulocyte 12/15-Lipoxygenase as Anti-Stroke Therapies

Ganesha Rai,[‡,‖] Netra Joshi,[§,‖] Joo Eun Jung,[†,‖] Yu Liu,[†,‖] Lena Schultz,[‡] Adam Yasgar,[‡] Steve Perry,[§] Giovanni Diaz,[§] Qiangli Zhang,[§] Victor Kenyon,[§] Ajit Jadhav,[‡] Anton Simeonov,[‡] Eng H. Lo,[†] Klaus van Leyen,*[,†] David J. Maloney,*[,‡] and Theodore R. Holman*[,§]

[†]Neuroprotection Research Laboratory, Department of Radiology, Massachusetts General Hospital, Harvard Medical School, Charlestown, Massachusetts 02129, United States

[‡]National Center for Advancing Translational Sciences, National Institutes of Health, 9800 Medical Center Drive, MSC 3370, Bethesda, Maryland 20892, United States

[§]Department of Chemistry and Biochemistry, University of California—Santa Cruz, Santa Cruz, California 95064, United States

S *Supporting Information*
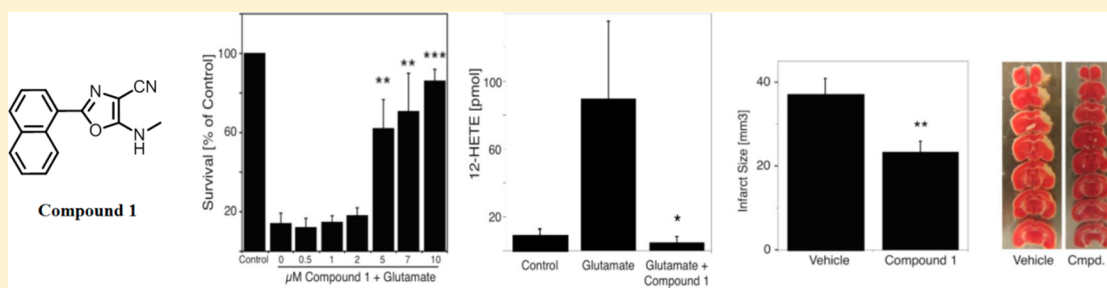
ABSTRACT: A key challenge facing drug discovery today is variability of the drug target between species, such as with 12/15-lipoxygenase (12/15-LOX), which contributes to ischemic brain injury, but its human and rodent isozymes have different inhibitor specificities. In the current work, we have utilized a quantitative high-throughput (qHTS) screen to identify compound **1** (**ML351**), a novel chemotype for 12/15-LOX inhibition that has nanomolar potency (IC_{50} = 200 nM) against human 12/15-LOX and is protective against oxidative glutamate toxicity in mouse neuronal HT22 cells. In addition, it exhibited greater than 250-fold selectivity versus related LOX isozymes, was a mixed inhibitor, and did not reduce the active-site ferric ion. Lastly, **1** significantly reduced infarct size following permanent focal ischemia in a mouse model of ischemic stroke. As such, this represents the first report of a selective inhibitor of human 12/15-LOX with demonstrated in vivo activity in proof-of-concept mouse models of stroke.

INTRODUCTION

Human lipoxygenases (LOX) are nonheme iron-containing enzymes that catalyze the dioxygenation of 1,4-*cis,cis*-pentadiene-containing polyunsaturated fatty acids (e.g., linoleic acid (LA) and arachidonic acid (AA)) to form hydroperoxy fatty acids.[1,2] The nomenclature of the LOX isozymes is loosely based on the carbon position (e.g., 5, 12, or 15) at which they oxidize arachidonic acid to form the corresponding hydroperoxyeicosatetraenoic acid (HpETE),[3] which is reduced to the hydroxyeicosatetraenoic acid (HETE) by intracellular glutathione peroxidases.[4] Human lipoxygenases and their metabolites have been implicated in numerous diseases. 5-LOX has been implicated in cancer,[5] asthma,[6,7] COPD,[8] allergic rhinitis,[9] osteoarthritis,[10,11] and atherosclerosis,[12–14] whereas platelet-type 12-LOX has been implicated in diabetes,[15,16] blood coagulation,[17] psoriasis,[18] and cancer.[19,20] Human reticulocyte 15-lipoxygenase-1 (12/15-LOX, aka 15-LOX-1) is also an attractive therapeutic target, particularly for its role in atherogenesis,[21,22] diabetes,[23–28] Alzheimer's disease,[29–31] new-born periventricular leukomalacia,[32] breast cancer,[33] and stroke,[34,35] with the latter being the focus of this work.

Stroke is the fourth-leading cause of death in the United States and the leading cause of disability.[36,37] However, only tissue plasminogen activator (tPA) is an FDA-approved drug treatment, and it is used in less than 5% of stroke patients. Therefore, a novel target for stroke therapy is highly desirable. The first reports of the contributions of 12/15-LOX to neuronal cell death in oxidative stress models were published starting in the late 1990s.[38–41] Because oxidative stress is a major neurodegenerative process in ischemic diseases such as stroke, a role for 12/15-LOX in stroke-induced brain injury seemed reasonable and, indeed, was found.[42–44] Later work showed that 12/15-LOX was detrimental not only to neurons but also to the brain vasculature after stroke[45] via a mechanism that involves an intracellular attack on mitochondria and
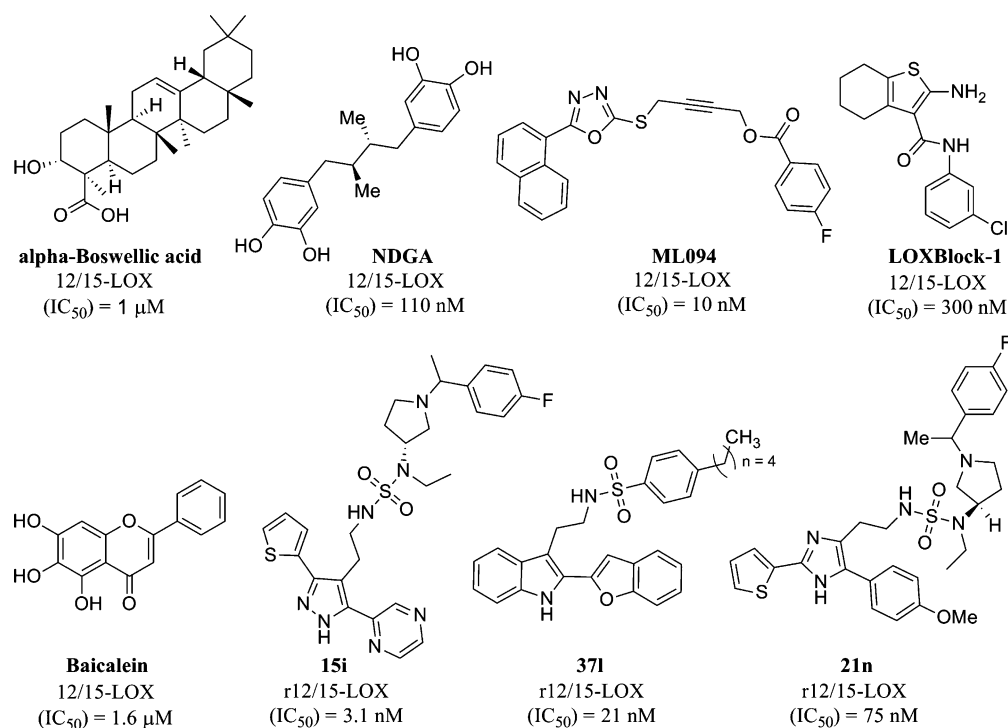
Figure 1. Examples of previously reported human 12/15-LOX (12/15-LOX) and rabbit 12/15-LOX (r12/15-LOX) inhibitors.

translocation of the apoptosis-inducing factor (AIF) to the nucleus.[46−48] Recent studies have shown that 12/15-LOX is also increased in human stroke.[34] In line with these findings, several LOX inhibitors have been found to reduce infarct size,[34,42,43] leakage of the blood brain barrier and edema formation,[45] and even hemorrhagic transformation following infusion of tPA.[34]

Consequently, these broad implications of 12/15-LOX in stroke regulation emphasize the need for small molecule inhibitors that effectively cross the blood brain barrier and target affected tissue. However, an additional aspect that must be considered in discovering human 12/15-LOX inhibitors is interspecies variability. The gene for 12/15-LOX for both humans and mice is termed ALOX15, reflecting the close homology (around 78%) and functional equivalence in both species. 12/15-LOX isozymes can oxidize both C12 and C15, forming 12-HpETE or 15-HpETE, respectively; however, the dominant product varies between species, with several isozymes oxidizing AA at C12, leading to a somewhat confusing nomenclature. The 12/15-LOX isozymes targeted here have historically been called 15-LOX, 15-LOX-1, or 15-LO-1 in humans and L-12-LOX, leukocyte-type 12-LO, or L-12-LO in mice. The number prefix reflects the preference for 15-HETE generation by human 12/15-LOX, whereas the preference is mostly for 12-HETE production for mouse 12/15-LOX. Unfortunately, this difference in substrate specificity could mean that an isoform-specific inhibitor that is selective toward human 12/15-LOX may not target the orthologous mouse 12/15-LOX, which would preclude the use of small animal stroke models. Considering that drug discovery relies to a large extent on rodent models of disease because of availability and cost, which is compounded by ethical considerations, it is therefore of great importance to identify bioactive compounds that target 12/15-LOX in both rodents and humans.

Over the last 12 years, our laboratory[49−56] and others[57−60] have attempted to identify potent and selective human 12/15-

LOX inhibitors, which has been met with limited success. Unfortunately, many of these inhibitors are reductive and/or promiscuous, such as boswellic acid (IC$_{50}$ = 1 μM),[61] nordihydroguaiaretic acid (NDGA) (IC$_{50}$ = 0.11 μM),[51] and baicalein (IC$_{50}$ = 1.6 μM),[55] as shown in Figure 1. Computational docking methods have been used to identify novel, nonreductive inhibitors, but the potency and selectivity of these compounds is limited (LOXBlock-1, Figure 1).[49] The most drug-like 12/15-LOX inhibitors that had been published prior to our investigations were those reported by researchers at Bristol-Myers Squibb (BMS) as well as Parke-Davis (now Pfizer) compound PD146176.[62] The BMS team identified tryptamine-based compounds (37l),[58] imidazole-based compounds (21n),[59] and pyrazole-based compounds (15i),[57] as shown in Figure 1. These inhibitors exhibited low nanomolar potency versus rabbit 12/15-LOX (r12/15-LOX) and modest selectivity against both 5-LOX and 12-LOX, but they had generally unfavorable physical properties (e.g., solubility and LogP)[57−59] and unacceptable PK properties for use in vivo. Most importantly, none of the above inhibitors, with the exception of LOXBlock-1, were screened in parallel against mouse 12/15-LOX, so it is unlikely that any would be amenable to stroke drug development.
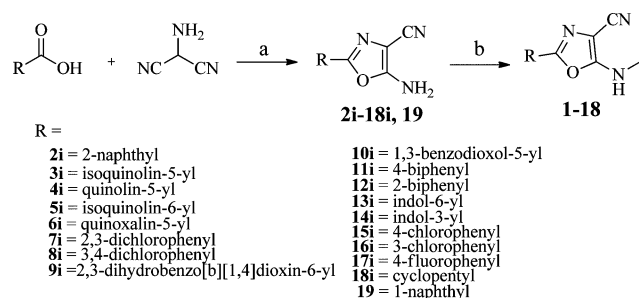
Our previously discovered inhibitor, LOXBlock-1 (Figure 1), demonstrated good activity in mouse models for stroke;[34] however, it is nonselective,[49] suggesting that the identification of novel selective inhibitors to interrogate 12/15-LOX biology in vivo is desirable. From our original quantitative high-throughput screen (qHTS) of 74 290 small molecules, the 1,3,4-oxadiazole-2-thiol chemotype (ML094, Figure 1)[56] was optimized for nanomolar potency and selectivity; however, we were unable to observe activity of ML094 in a cellular context.[56] Therefore, in this work, we present our efforts to identify a specific 12/15-LOX inhibitor that is potent against both the human and the mouse homologues of 12/15-LOX. As such, we rescreened our top hits from the original HTS with

our cellular mouse model of oxidative stress-related cell death[38] and discovered a novel oxazole-4-carbonitrile core scaffold. We discuss the SAR and biological activity of this novel scaffold, which has nanomolar potency against human 12/15-LOX, selectivity over related eicosanoid producing enzymes, and potency against mouse 12/15-LOX in both a cellular and an in vivo model of stroke.

■ CHEMISTRY

Compounds **1**−**18** in Table 1 were synthesized as shown in Scheme 1. Intermediates **2i**−**18i** and **19** were obtained by

Scheme 1. Synthetic Route to Compounds 1−18[a]

R =
2i = 2-naphthyl
3i = isoquinolin-5-yl
4i = quinolin-5-yl
5i = isoquinolin-6-yl
6i = quinoxalin-5-yl
7i = 2,3-dichlorophenyl
8i = 3,4-dichlorophenyl
9i = 2,3-dihydrobenzo[b][1,4]dioxin-6-yl

10i = 1,3-benzodioxol-5-yl
11i = 4-biphenyl
12i = 2-biphenyl
13i = indol-6-yl
14i = indol-3-yl
15i = 4-chlorophenyl
16i = 3-chlorophenyl
17i = 4-fluorophenyl
**18i** = cyclopentyl
19 = 1-naphthyl

[a]Reagents and conditions: (a) T$_3$P, NEt$_3$, EtOAc, rt, 12 h; (b) paraformaldehyde, NaOMe, MeOH, 65 °C, 1 h, then NaBH$_4$, rt, 1 h.

propylphosphonic anhydride (T$_3$P)-assisted coupling of the corresponding commercially available carboxylic acids with 2-aminomalanonitrile followed by cyclization in one step. This modified synthesis of 5-amino-2-substituted-1,3-oxazole-4-carbonitriles allows facile access to a variety of compounds via a simple workup and purification from commercially available carboxylic acids. Because of the low nucleophilicity of the amine group, our initial attempts to monomethylate the 5-amino-2-substituted-1,3-oxazole-4-carbonitrile intermediate with several known methylation methods including methyl iodide, formic acid, or methyl boronic acid were met with limited success. However, condensation with paraformaldehyde in the presence of sodium methoxide in methanol followed by in situ reduction with sodium borohydride afforded required products **1**−**18** in modest yields.

Scheme 2 represents the general methodology utilized for the synthesis of compounds listed in Table 2. Toward this end, 5-amino-2-(naphthalen-1-yl)oxazole-4-carbonitrile **19** was converted to an advanced intermediate (**19a**) via Sandmeyer reaction by treating with *t*-butyl nitrite in the presence of copper(II) chloride. Heating the various amines to reflux with intermediate **19a** in THF afforded required analogues **20**−**26** and **28**−**31**. Compound **27** was obtained via acetylation of intermediate **19** with acetic anhydride and cat. DMAP.
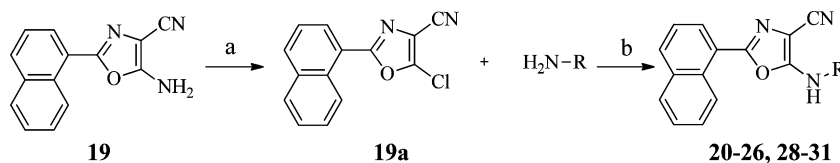
The synthesis of compounds **32**−**40** (Table 3) is outlined in Scheme 3. Analogues **32**−**34** were prepared via chlorination of intermediates **32a**−**34a** with hexachloroethane in the presence of LDA followed by condensation with methylamine. Amination of 5-chloro-2-(naphthalen-1-yl)thiazole-4-carbonitrile (**32b**) required microwave heating in a polar solvent, such as 2-propanol, for complete conversion of the starting material. The details of the synthesis of intermediate **32a**[63,64] are described in the Supporting Information. Intermediates **33a** and **34a** were synthesized following the literature protocols described for similar compounds. The reaction of 4-methyl-3-thiosemicarbazide with 1-naphthoic acid in the presence of EDC furnished oxadiazole analogue **35**, but, surprisingly, when T$_3$P coupling conditions were used, only thiadiazole analogue **36** was formed. Synthesis of compound **37** was accomplished utilizing a Cornforth rearrangement of intermediate **37b**, which was prepared from intermediate **37a** by coupling with methylamine, as shown in Scheme 3. Intermediate **37a** was prepared according to a known protocol reported to similar compounds in the literature.[65] The synthesis of analogue **38** from 1-naphthyl boronic acid and intermediate **38a** using classical Suzuki conditions was met with limited success.[66] Gratifyingly, the Suzuki coupling reaction was moderately successful using a silica-bound DPP-Pd catalyst (SiliaCat-DPP-Pd) under reflux conditions over 24 h. Synthesis of intermediates **39a**−**40a** was accomplished using a Pd(PPh$_3$)$_4$-catalyzed microwave-assisted regioselective Suzuki coupling between 1-naphthyl boronic acid and 2,6-dichloro pyridine or pyrimidine derivative, respectively. Subsequent condensation of these intermediates with methylamine furnished desired analogues **39**−**40** following HPLC purification.

■ RESULTS AND DISCUSSION

To investigate structural requirements for optimal 12/15-LOX inhibition, we conducted a SAR study of the lead molecule, as shown in Tables 1−3 (**1**−**40**). Initially, the 1-naphthyl group on the left side of the molecule was replaced with various aryl and heterocyclic groups, as shown in Table 1. The bioisosteric replacement of 1-naphthyl with 2,3-dichlorophenyl (**7**) or 3,4-dichlorophenyl (**8**) groups showed comparable, albeit slightly lower, potencies than **1** (IC$_{50}$ = 0.46, 0.81, and 0.20 μM, respectively). Replacement with a 2-naphthyl group showed reduced potency (**2**, IC$_{50}$ > 30 μM) compared to the 1-naphthyl substitution, which, on the basis of space-filling analysis, agreed with the findings we observed for dichloro analogues **7** and **8**. Several other modifications, including saturated rings or heterocyclic rings at this region (**3**−**6** and **9**−**18**), also resulted in reduced potency. Thus, in general, the 1-naphthyl group appeared to be optimal for 12/15-LOX inhibition, as variations in size and electrostatics in this region were not well tolerated. Accordingly, the 1-naphthyl group was

Scheme 2. Synthetic Route to Compounds 20−26 and 28−31[a]

[a]Reagents and conditions: (a) CuCl$_2$, *t*-BuNO$_2$, MeCN, 25 °C, 3 h, 35%; (b) THF, reflux, 1−12 h.

Scheme 3. Synthetic Route to Compounds 32–40[a]
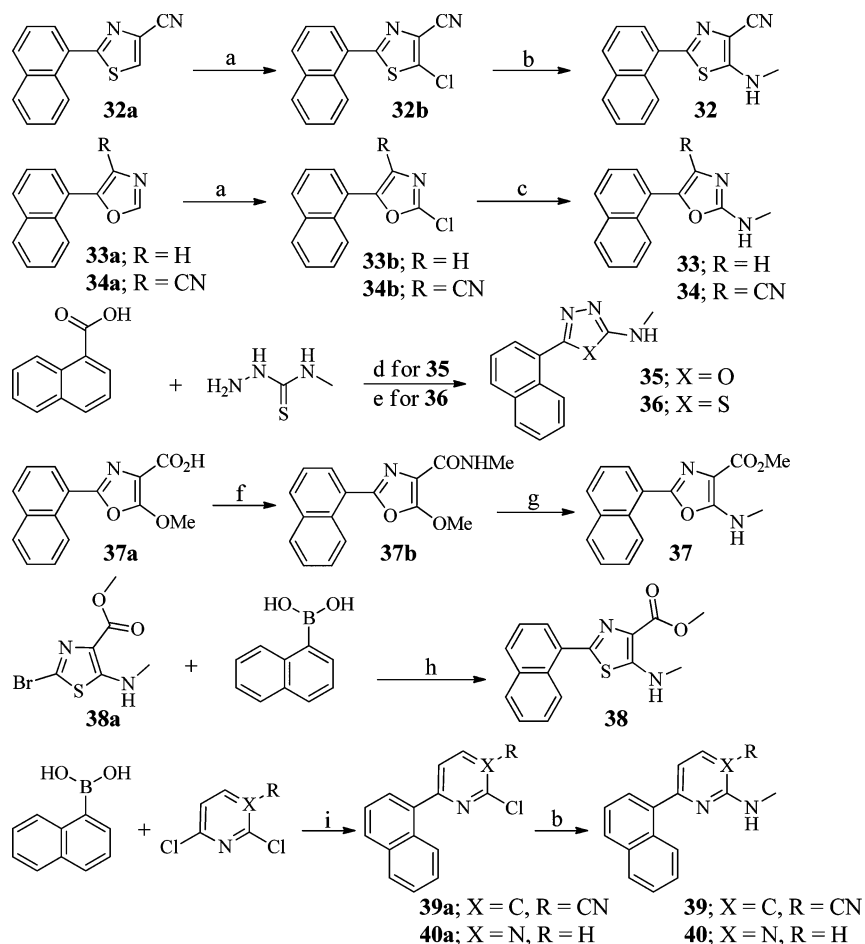
[a]Reagents and conditions: (a) C$_2$Cl$_6$, LDA, THF, −78 °C, 2–4 h; (b) CH$_3$NH$_2$, i-PrOH, microwave, 120 °C, 0.5 h; (c) CH$_3$NH$_2$, THF, 65 °C, 1–2 h; (d) EDC, DMF, 25 °C, 12 h; (e) T$_3$P, NEt$_3$, DMF, 25 °C, 6 h; (f) (1) (COCl)$_2$, CH$_2$Cl$_2$, (2) CH$_3$NH$_2$, NEt$_3$, CH$_2$Cl$_2$, 25 °C, 1 h; (g) toluene, 110 °C, 12 h; (h) SiliaCat-DPP-Pd, Na$_2$CO$_3$, DME, 105 °C, 24 h; (i) Pd(PPh$_3$)$_4$, Na$_2$CO$_3$, DME, microwave, 150 °C, 45 min.

held constant while other regions of the molecule were explored for further SAR (Tables 2 and 3).

Having explored modifications to the 1-naphthyl moiety, our next focus was to explore modifications of the *N*-methyl side chain at the 5-position, as shown in Table 2 (19–31). Removal of the methyl group drastically reduced potency (19, IC$_{50}$ = 25 μM), and dimethylation reduced potency as well (20, IC$_{50}$ > 30 μM). Modifications of the methyl group with other alkyl substitutions, such as ethyl, *n*-propyl, *n*-butyl, and *n*-pentyl groups, were tolerated (21–24), with comparable or even improved potency being observed. However, replacing the methyl group with a branched alkyl group (26) or heterocyclic groups (30–31) significantly reduced the potency. Larger groups, such as benzyl- (28, IC$_{50}$ > 30 μM) or phenyl-substituted analogues (29, IC$_{50}$ > 30 μM), also showed diminished 12/15-LOX activity. Overall, these data suggest that the monoalkylation with straight-chain alkyl groups is critical for optimal 12/15-LOX inhibition.

Lastly, we turned our attention to optimization of the 1,3-oxazole core and its various substituents (Table 3). Replacing the 1,3-oxazole core with a 1,3-thiazole ring (32, IC$_{50}$ = 0.55 μM) resulted in a 2-fold decrease in potency. This result could be partly attributed to the difference in size and hardness/softness of the sulfur and oxygen atoms in the thiazole and oxazole rings, respectively. The diminished potency trend

continued further for the pyridine (39, IC$_{50}$ > 40 μM) and pyrimidine analogues (40, IC$_{50}$ > 40 μM). Attempts to mimic the interaction of the oxazole core were largely unsuccessful with the *N*-methyl/oxadiazole derivative (35, IC$_{50}$ = 5.4 μM) or the thiadiazole analogue (36, IC$_{50}$ > 40 μM). Interchanging the positions of the 1-naphthyl group and the -NHMe group (analogues 33–34) also led to complete loss of activity. In summary, this chemotype showed very tight SAR, and our efforts to make several changes around the lead molecule resulted in similar or lower potency, with the exception of analogues 21–23, which showed marginally improved potency.

Biological Evaluation of ML351. Concurrently with the SAR investigations against human 12/15-LOX in vitro, we investigated the potency of **1** against mouse 12/15-LOX, utilizing a neuronal cell-based assay. Glutamate-induced oxidative stress[67−69] leads to time-dependent cell death mediated by 12/15-LOX in both immature primary neurons and mouse hippocampal HT22 cells.[38,46,70] Primary neurons require a lengthy isolation procedure and also show relatively modest increases in cell death in this assay, indicating that they are not suited for a high-throughput testing approach. In contrast, HT22 cells grow quickly and consistently feature low cell death under control conditions, but a majority of cells die after glutamate treatment (50−100%). We have now adapted this assay to 96-well plates, allowing for moderate-to-high

Table 1. Variations to Compound 1 (Analogues 2−18)[a]
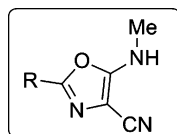
Compound	R	IC$_{50}$ (μM) [± SD (μM)]	Compound	R	IC$_{50}$ (μM) [± SD (μM)]
1		0.20 [0.04]	10		7.6 [2]
2		>30[b]	11		>40
3		>30[b]	12		23 [13]
4		3.6 [0.5]	13		>40
5		0.73	14		3.9 [0.2]
6		>40	15		25 [4]
7		0.46 [0.06]	16		6.3 [0.5]
8		0.81 [0.2]	17		15 [1]
9		>40	18		>50

[a]IC$_{50}$ values represent the half-maximal (50%) inhibitory concentration, as determined in the UV−vis cuvette-based assay in triplicate. [b]Compound possessed low efficacy, with less than 50% maximal inhibition at 25 μM inhibitor.

throughput against the screened compounds. The characteristic Z′ score used to evaluate the technical quality and suitability of this approach as a screening tool averaged 0.77 over 10 experiments (SD = 0.13; range = 0.49−0.94), where values above 0.5 indicate an excellent assay.[71]

To verify that inhibition of oxidative stress-related cell death in HT22 cells is indeed a good measure of the efficacy of a given inhibitor against the mouse 12/15-LOX, we decided to reinvestigate the characteristics of cell injury in this model. Levels of the mouse 12/15-LOX product, 12-HETE, are known to be increased in the mouse brain following ischemia,[34] and they are also elevated by glutamate treatment of HT22 cells.[34,38] We used HPLC/MS to measure 12-HETE secreted to the medium from cells incubated under control conditions or treated with glutamate as well as cotreated with several compounds with or without inhibitory activity for mouse 12/15-LOX. Following exclusion of one outlier with extremely high 12-HETE (but also high levels of cell death), there was a good correlation between cell death and levels of 12-HETE secreted: when 12-HETE levels were high, there was increased cell death, and when 12-HETE levels were low, there was little cell death (Figure 2A). Interestingly, levels of 15-HETE were also increased in the medium of glutamate-treated HT22 cells to a similar extent as 12-HETE (Figure 2B). This was surprising because mouse 12/15-LOX is generally thought to make only minor amounts of 15-HETE, typically less than 20% of the 12-HETE generated. Nonetheless, 15-HETE production was also

blocked by 12/15-LOX inhibitors that protected HT22 cells and reduced 12-HETE levels, indicating that both arachidonic acid metabolites were made by the same enzyme. It is unclear why this large amount of 15-HETE was generated, and we are currently working on a different line of research to address this important result.

Upon testing of compound 1 in HT22 cells, we found a dose-dependent protection against oxidative glutamate toxicity (Figure 3A). To verify the on-target efficacy of 1, we also measured 12-HETE secreted from the cells. The increase in 12-HETE following glutamate treatment was completely reversed by incubation in the presence of 10 μM of 1 (Figure 3B). These results suggest that 1 is capable of reaching its target in the cell and effectively inhibiting mouse 12/15-LOX, albeit with lower affinity than seen against human 12/15-LOX in vitro (IC$_{50}$ = 200 nM).

In addition to analogues that were active in vitro against human 12/15-LOX, we also tested several inactive analogues (11, 31, and 34) in HT22 cells, with the goal of identifying a good negative control (Figure 4). Surprisingly, 11 and 31 featured similar protective qualities at 5 μM, suggesting that they are able to inhibit the mouse homologue of 12/15-LOX even though they are inactive against human 12/15-LOX. In contrast, 5 μM of 34 did not protect HT22 cells, suggesting that it is inactive against both human and mouse 12/15-LOX and is a suitable negative control for 1. These data re-emphasize the importance of screening 12/15-LOX inhibitors against both
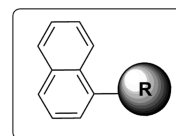
Table 2. Variations to Compound 1 (Analogues 19−31)[a]
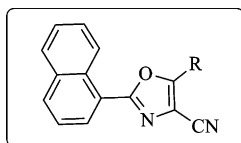
Compound	R	IC$_{50}$ (μM) [± SD (μM)]
1	NHMe	0.20 [0.04]
19	NH$_2$	25 [10]
20	N(Me)$_2$	>30[b]
21	HN⌒	0.12 [0.3]
22	HN⌒⌒	0.10 [0.3]
23	HN⌒⌒⌒	0.12 [0.05]
24	HN⌒⌒⌒⌒	0.3 [0.04]
25	HN⌒⌒	3.0 [1]
26	HN⌁	>40
27	NHAc	10 [3]
28	HN⌒Ph	>30[b]
29	HN·Ph	>30[b]
30	HN–⌁O	>25
31	HN–⌁NH	>40

[a]IC$_{50}$ values represent the half-maximal (50%) inhibitory concentration, as determined in the UV−vis cuvette-based assay in triplicate. [b]Compound possessed low efficacy, with less than 50% maximal inhibition at 25 μM inhibitor.

Table 3. Variations to Compound 1 (Analogues 32−40)[a]

Compound	R	IC$_{50}$ (μM) [± SD (μM)]
1	(oxazole, NHMe, CN)	0.20 [0.04]
32	(thiazole, NHMe, CN)	0.55 [0.06]
33	(oxazole, NHMe)	>40
34	(oxazole, NHMe, NC)	>40
35	(oxadiazole, NHMe)	5.4 [1.8]
36	(thiadiazole, NHMe)	>40
37	(oxazole, NHMe, OMe, O)	>40
38	(thiazole, NHMe, OMe, O)	>30[b]
39	(pyridine, CN, NHMe)	>40
40	(pyrimidine, NHMe)	>40

[a]IC$_{50}$ values represent the half-maximal (50%) inhibitory concentration, as determined in the UV−vis cuvette-based assay in triplicate. [b]Compound possessed low efficacy, with less than 50% maximal inhibition at 25 μM inhibitor.

human and mouse 12/15-LOX because activity against one species does not guarantee activity or inactivity against the other.

Upon the determination that **1** was potent against both in vitro human 12/15-LOX and ex vivo mouse 12/15-LOX (HT22 cell assay), we then investigated the selectivity of a few of our top analogues against related human LOX isozymes (5-LOX, 12-LOX, and 15-LOX-2). Of the four 12/15-LOX inhibitors tested, **1**, **7**, **8**, and **32**, all displayed excellent selectivity against all three isozymes (IC$_{50}$ > 50 μM, Supporting Information, Table S1). We were encouraged by these findings because few compounds reported in the literature have achieved nanomolar potency toward 12/15-LOX while maintaining excellent selectivity toward other isozymes. Moreover, we investigated whether these analogues inhibited cyclooxygenase-1 (COX-1) and/or COX-2 and determined that none of them displayed inhibition (<10% at 15 μM).

Mechanistic Investigations of Compound 1. LOX inhibitors are known to exhibit a variety of inhibitory mechanisms, such as chelative, reductive, or competitive. The UV−vis pseudoperoxidase activity assay was therefore performed on four selected analogues (**1**, **7**, **8**, and **32**; Supporting Information, Table S1) to determine if the mechanism was reductive in nature. It was observed that the hydroperoxide product was not degraded, 12/15-LOX was not irreversibly inhibited, and there was no elongation of the enzymatic lag phase (data not shown). These data are

consistent with a nonreductive inhibitory mechanism. To investigate the nature of inhibition further, steady-state kinetics were performed using compound **1** by monitoring the formation of 15-HpETE as a function of substrate and inhibitor concentration in the presence of 0.01% Triton X-100. Replots of K_m/V_{max} and $1/V_{max}$ versus inhibitor concentration yielded linear plots (Supporting Information, Figure S2), with K_i equaling 0.1 ± 0.002 μM and K_i' equaling 1.2 ± 0.02 μM. These parameters are defined as the equilibrium constants of dissociation from the catalytic (K_i) and secondary sites (K_i'), respectively. The K_i value is in good agreement with the IC$_{50}$ value, and because of the greater than 10-fold difference between K_i and K_i', we assume the secondary site to be the allosteric site,[72,73] which is consistent with our previous studies of 12/15-LOX inhibition.[56]

In Vitro ADME and in Vivo PK Profile. Our previously reported small molecule inhibitor for 12/15-LOX inhibition, **ML094**, demonstrated excellent potency and selectivity but lacked sufficient solubility, cell permeability, and microsomal stability ($t_{1/2}$ < 2 min).[56] Moreover, this compound possessed
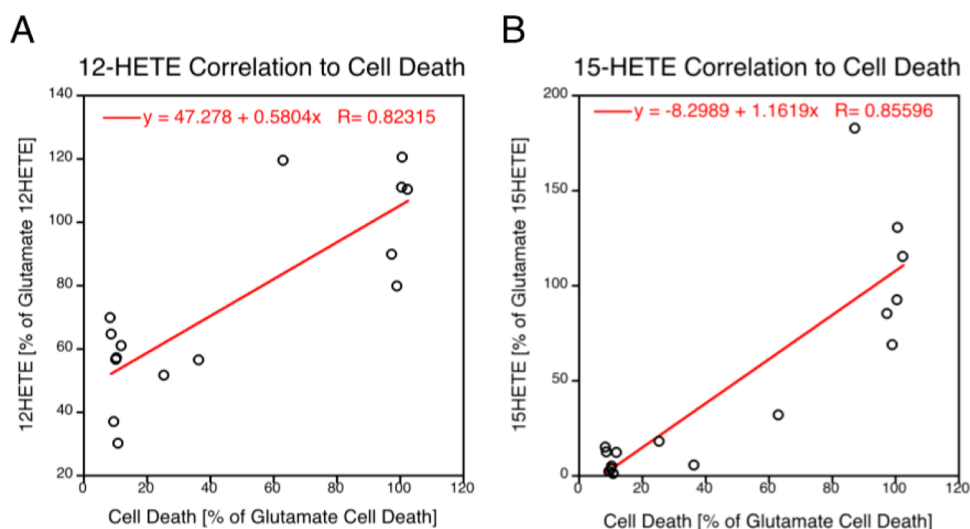
Figure 2. Correlation between arachidonic acid metabolites and cell death. (A) 12-HETE, which is graphed as the percent of 12-HETE secreted from glutamate-treated cells vs the percent of cell death in glutamate-treated samples. (B) Positive correlation between 15-HETE and cell death.
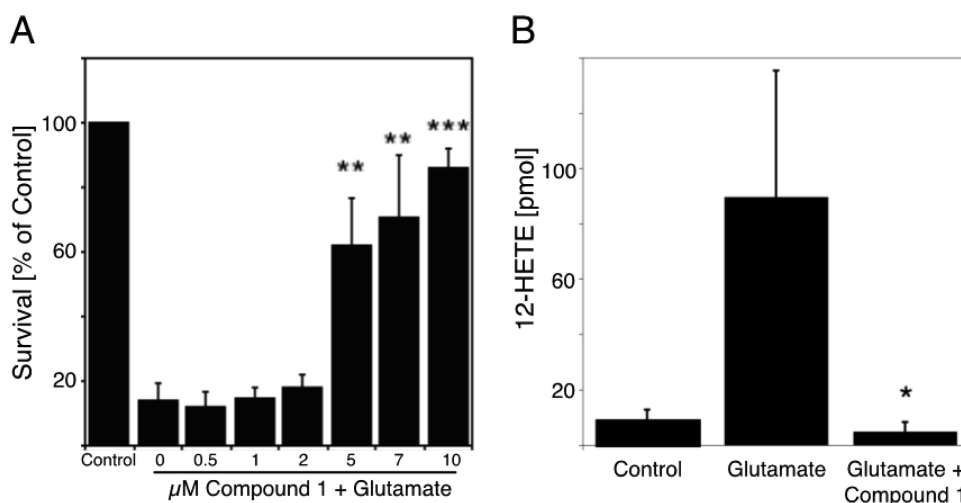

Figure 3. (A) Protection against glutamate-induced HT22 death by increasing amounts of **1** (** $p < 0.01$ and *** $p < 0.001$ vs glutamate only). (B) Inhibition of 12-HETE in HT22 cells by 10 μM of **1** following treatment with 5 mM glutamate (* $p < 0.05$ vs glutamate only).
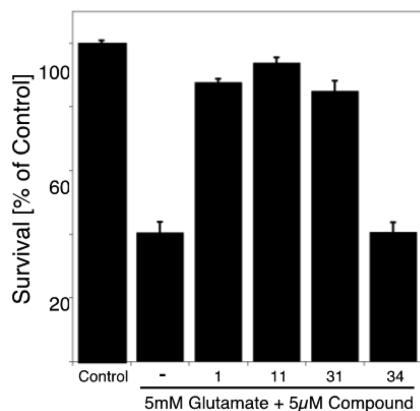

Figure 4. Cellular protection at 5 μM of **1** and some analogues in HT22 cells. Despite not inhibiting human 12/15-LOX, **11** and **31** show similar protection to **1**, indicating that they inhibit the mouse enzyme, whereas **34** does not protect HT22 cells.

an essential ester moiety that could be susceptible to intracellular and plasma esterases, rendering it inactive and

possibly limiting its utility in advanced biological models. Thus, we were encouraged by the in vitro ADME (Table 4) and in vivo PK properties (Table 5) of **1**, as they represent a vast improvement over the majority of compounds reported previously (vide infra). The majority of the compounds possess a low molecular weight (e.g., 249 Da) and a favorable log D (pH 7.4) between 2 and 3, which was obtained by Analiza Inc. using their scaled-down shake flask lipophilicity method, yet most analogues have poor solubility. The aqueous kinetic solubility in PBS buffer (pH 7.4) was determined to be 1.2 μM, which is about 7 times the in vitro IC$_{50}$ value. Empirically, we did observe a vast improvement in the solubility in the 15-LOX assay buffer (data not shown), which was encouraging and suggests that solubility was not a detrimental factor in the biochemical studies. Importantly, the compound demonstrated favorable PAMPA permeability (passive) and acceptable Caco-2 permeability of >1 (1.5 cm/s^{-6}), with no evidence of efflux (efflux ratio: 0.7), indicating that the compound is not susceptible to the action of P-glycoprotein 1 (Pgp), a well-characterized ABC transporter. Moreover, **1** was stable in various aqueous solutions (pH 2, 7.4, and 9) (see Supporting

Table 4. ADME Profile for 1[a]

compound	kinetic solubility (μM)[b]	microsomal stability $t_{1/2}$ (min)[c]	CYP 2D6 inhibition at 3 μM[d]	CYP 3A4 inhibition at 3 μM[e]	permeability (10^{-6} cm/s)		mouse plasma stability remaining at 2 h
1	1.2	18 (rat) 5.5 (mouse)	10.30%	3.50%	723 (PAMPA)	1.5 (Caco-2)	100%

[a]All experiments were conducted at Pharmaron Inc. [b]In PBS buffer (pH 7.4). [c]Represents the stability in the presence of NADPH. The probe compound showed no degradation without NADPH present over a 1 h period. [d]Dextromethorphan was used as the substrate. [e]Midazolam was used as the substrate.

Table 5. In Vivo PK (Mouse) of 1 at 30 mg/kg IP[a]

compound[b]	tissue	$t_{1/2}$ (h)	t_{max} (h)	C_{max} (μM)	AUC_{inf} (μM h)	brain/plasma[c]
1	plasma	1.1	0.25	13.8	13	2.8
	brain	1	0.5	28.8	35.5	

[a]All experiments were conducted at Pharmaron Inc. using male CD1 mice (6−8 weeks of age). Data was collected in triplicate at eight time points over a 24 h period. [b]Formulated as a solution (10% Solutol, 10% Cremophor EL, and 20% PEG 400 in saline). [c]Brain/plasma ratio [AUC_{last}(brain)/AUC_{last}(plasma)].

Information) and mouse plasma (Table 4). In addition, **1** exhibited minimal CYP inhibition of the 2D6 and 3A4 isoforms at 10.3 and 3.5% inhibition, respectively. Microsomal stability appears to be species-dependent, with **1** possessing modest stability to rat liver microsomes (18 min) while being less stable to mouse liver microsomes (5.5 min). The compounds were completely stable in the absence of NADPH, suggesting CYP-mediated degradation. Given our plan to test compound **1** in proof-of-concept (POC) mouse models of stroke, we also obtained in vivo PK data on **1** (Table 5) and found a suitable formulation for **1** (10% Solutol, 10% Cremophor EL, and 20% PEG400 in saline). As anticipated from the microsomal stability studies, **1** has a fast half-life in both plasma and brain ($t_{1/2} \sim 1$ h), with a C_{max} of 13.8 μM in plasma and 28.8 μM in brain. Encouragingly, **1** has a brain/plasma ratio of 2.8, which demonstrates favorable blood−brain barrier permeability and suggests that this compound is suitable for in vivo POC models of ischemic stroke (vide infra).

Cell Activity and in Vivo Efficacy. After establishing the SAR profile against recombinant human 12/15-LOX, determining the efficacy of **1** in our cellular mouse 12/15-LOX assay, and measuring its in vitro ADME/in vivo PK properties, we then sought to determine its efficacy in mouse models of ischemic stroke. For these initial studies, we chose the permanent focal ischemia model in mice, which has been shown to mimic the pathophysiological mechanisms following ischemic injury.[74] The advantage of this model is that it does not inflict surgical trauma and has a low mortality compared to other methods. The thrombosis event in the middle cerebral artery (MCA) is induced by topical application of FeCl$_3$ to the intact dura mater, leading to a cortical infarct. Laser doppler flowmetry was used to monitor blood flow reduction, and infarct size was measured following sacrifice at 24 h by staining of 1 mm thick brain slices with 2,3,5-triphenylterazolium hydrochloride (TTC). IP administration of **1** given 2 h after the induced ischemia resulted in a ∼30% reduction in infarct size ($p < 0.01$), demonstrating efficient neuroprotection in this mouse model of permanent focal ischemia (Figure 5).

CONCLUSIONS

12/15-LOX contributes to neuronal cell death in oxidative stress models[38−44] and is also detrimental not only to neurons but also to the brain vasculature after stroke[45] via intracellular attack on mitochondria and translocation of AIF to the nucleus.[46−48] Moreover, the protein level of 12/15-LOX
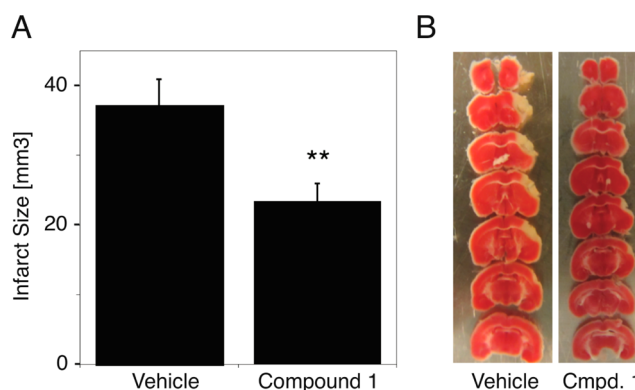

Figure 5. (A) Activity of compound **1** (50 mg/kg) administered IP in a mouse distal middle cerebral artery occlusion (MCAO) model of permanent focal ischemia (** $p < 0.01$). (B) Typical examples of sequential (top to bottom represents front to back sections of a single brain, respectively) TTC-stained brain sections from vehicle- and compound **1**-treated mice. The white areas in the cortex (top right) indicate nonviable infarcted tissue.

gradually increases over time after experimental stroke,[47] providing an opportunity for therapeutic intervention. Our initial efforts to identify a stroke-relevant 12/15-LOX inhibitor proved to be unsuccessful because of its inactivity in our mouse ex vivo model, resulting from either cellular inactivation or inactivity against mouse 12/15-LOX.[56] Fortunately, reinterrogation of the HTS data along with simultaneous cellular mouse 12/15-LOX screening revealed another 12/15-LOX inhibitor (**1**) with better drug-like properties and, more importantly, mouse ex vivo activity. Our initial medicinal chemistry efforts, described herein, provided important SAR to guide future investigations, but we were unable to improve potency significantly, and the tolerability for the structural changes is limited. The most significant loss of inhibition was observed at the 1-naphthyl position, where almost all substitutions resulted in significant loss in activity, with the exception of its bioisosteric dichloro analogues (**7** and **8**), which only showed a slight decrease in activity. Modifications of the methyl group on the *N*-methyl side chain were not well tolerated either, indicating that the straight-chain monoalkylated amine was critical for potency. Moreover, the only substitution tolerated for 1,3 oxazole core ring was the replacement with a 1,3-thiazole (**32**), which resulted in a 2-fold decrease in the potency. The cyanide group on the oxazole core was found to

be essential, with modifications to this group completely abolishing activity. Subsequent selectivity studies of **1** and related analogues revealed that these compounds have minimal activity toward 5-LOX, 12-LOX, 15-LOX-2, COX-1, and COX-2.

Most importantly, **1** was active in both protecting mouse neuronal cells (HT22) and in reducing the infarct size of stroke-induced mice. This is a significant discovery because identifying therapeutically useful specific inhibitors of 12/15-LOX is not trivial due to the differences between the human and mouse 12/15-LOX isozymes. Interestingly, we have identified analogues of compound **1** (**11** and **31**) that did not inhibit human 12/15-LOX but protected HT22 cells against oxidative stress. These might work in mice to protect against experimental stroke, yet in human stroke, they would most likely fail because of their inability to target human 12/15-LOX. The lesson to be drawn from this is that simply because a given inhibitor is selective for a LOX isoform in one species its efficacy cannot be readily extrapolated to other species. Moreover, the LOX isotype involved in a given process cannot be reliably inferred from inhibitor experiments without taking into account the species from which the cells were derived.

In conclusion, compound **1** is the first highly selective 12/15-LOX inhibitor active against human 12/15-LOX and mouse 12/15-LOX, as seen by its effectiveness in our mouse stroke model. This attribute of **1** is significant because it maintains the human 12/15-LOX selectivity, which is beneficial to a human therapeutic, but is also functional in a mouse stroke model, which is critical to developing its biological efficacy. Therefore, using our pipeline approach, we have identified a potent and selective inhibitor of human 12/15-LOX that is neuroprotective in a mouse model of stroke and therefore can be utilized in preclinical studies to develop it as a potential first-line stroke therapy.

■ EXPERIMENTAL SECTION

General Methods for Chemistry. All air- or moisture-sensitive reactions were performed under positive pressure of nitrogen with oven-dried glassware. Anhydrous solvents such as dichloromethane, *N,N*-dimethylforamide (DMF), acetonitrile, dioxan, dimethoxyethane, methanol, and triethylamine were purchased from Sigma-Aldrich. Tetrakis and a 50% of solution of T3P in DMF or ethyl acetate were purchased from Strem Chemicals and used as such. SiliaCat heterogeneous catalyst DPP-Pd (catalog no. R390-100) was purchased from SiliCycle Inc. Preparative purification was performed on a Waters semipreparative HPLC system using a Phenomenex Luna C18 column (5 μm, 30 × 75 mm) at a flow rate of 45 mL/min. The mobile phase consisted of acetonitrile and water (each containing 0.1% trifluoroacetic acid). A gradient of 10–50% acetonitrile over 8 min was used during the purification. Fraction collection was triggered by UV detection (220 nm). Analytical analysis was performed on an Agilent LC/MS (Agilent Technologies, Santa Clara, CA). Method 1: A 7 min gradient of 4–100% acetonitrile (containing 0.025% trifluoroacetic acid) in water (containing 0.05% trifluoroacetic acid) was used with an 8 min run time at a flow rate of 1 mL/min. A Phenomenex Luna C18 column (3 μm, 3 × 75 mm) was used at a temperature of 50 °C. Method 2: A 3 min gradient of 4–100% acetonitrile (containing 0.025% trifluoroacetic acid) in water (containing 0.05% trifluoroacetic acid) was used with a 4.5 min run time at a flow rate of 1 mL/min. A Phenomenex Gemini Phenyl column (3 μm, 3 × 100 mm) was used at a temperature of 50 °C. Method 3: Analysis was performed on an Agilent 1290 Infinity Series HPLC. UHPLC long gradient equivalent 4–100% acetonitrile (0.05% trifluoroacetic acid) in water was used over 3.5 min with a run time of 4 min and a flow rate of 0.8 mL/min. A Phenomenex Kinetex 1.7 μm C18 column (2.1 × 100 mm) was used at a temperature of 50 °C. Purity determination was performed using an Agilent diode array detector for methods 1–3. Mass determination was performed using an Agilent 6130 mass spectrometer with electrospray ionization in the positive mode. ^{1}H NMR spectra were recorded on Varian 400 MHz spectrometers. Chemical shifts are reported in ppm, with undeuterated solvent (DMSO-d_6 at 2.49 ppm) as internal standard for DMSO-d_6 solutions. All of the analogues tested in the biological assays have a purity greater than 95% on the basis of both analytical methods. High-resolution mass spectrometry was recorded on Agilent 6210 time-of-flight LC/MS system. Confirmation of molecular formula was accomplished using electrospray ionization in the positive mode with the Agilent Masshunter software (version B.02).

Experimental Procedures. *General Procedure for the Preparation of 5-Amino-2-substituted Oxazole-4-carbonitrile Intermediates (1i–18i and 19).* A mixture of carboxylic acid (5.77 mmol, 1 equiv) and 2-aminomalononitrile·TsOH (5.77 mmol, 1 equiv) in ethyl acetate (15 mL) was added NEt$_3$ (17.32 mmol, 3 equiv) followed by a 50% solution of T$_3$P in ethyl acetate (14.44 mmol, 2.5 equiv). The reaction was allowed to stir at room temperature for 12 h and was then diluted with ethyl acetate. The organic layer was successively washed with water, saturated bicarbonate solution, and brine. The organic layer was then dried with MgSO$_4$ and concentrated under reduced pressure. The crude product was purified on a biotage flash system, eluting with 50–100% ethyl acetate in hexanes containing 0.1% triethylamine to provide pure products.

General Procedure for the Preparation of 2-Substituted-5-(methylamino)oxazole-4-carbonitrile (1–18). A mixture of 5-amino-2-substituted oxazole-4-carbonitrile (1.79 mmol, 1 equiv), paraformaldehyde (0.11 g, 3.57 mmol, 2 equiv), and sodium methoxide (0.096 g, 1.79 mmol, 1 equiv) in methanol (10 mL) was stirred at 65 °C for 1 h until a clear mixture was obtained. The reaction mixture was cooled to room temperature, sodium borohydride (3.57 mmol, 2 equiv) was added slowly, and the mixture was stirred further at room temperature for 1 h. The crude product was extracted with ethyl acetate and successively washed with water and brine. The ethyl acetate layer was dried with MgSO$_4$ and concentrated under reduced pressure. The crude product was taken up in DMSO and purified on a reversed-phase HPLC system. Characterization data for key compounds is given below (see Supporting Information for details and characterization data for all other compounds)

5-(Methylamino)-2-(naphthalen-1-yl)oxazole-4-carbonitrile (1, ML351). This compound was prepared starting from 1-naphthoic acid and aminomalononitrile via intermediate **19** following the above general procedure. LC-MS retention time: (method 1) 6.011 and (method 2) 2.42 min. ^{1}H NMR (400 MHz, DMSO-d_6) δ 9.15 (dq, J = 8.7 and 0.9 Hz, 1H), 8.44 (brs, 1H), 8.10–7.99 (m, 3H), 7.74–7.57 (m, 3H), 3.07–3.01 (m, 3H). ^{13}C NMR (400 MHz, DMSO-d_6) δ 161.9, 161.9, 149.5, 134.1, 134.0, 131.2, 129.2, 128.3, 127.2, 127.2, 127.0, 126.9, 125.8, 125.8, 125.8, 125.7, 122.1, 116.5, 116.5, 84.1, 84.1, 84.1, 29.7, 29.7, 29.6. HRMS (ESI): m/z (M + H)$^+$ calcd for C$_{15}$H$_{12}$N$_3$O, 250.0975; found, 250.0975.

2-(2,3-Dichlorophenyl)-5-(methylamino)oxazole-4-carbonitrile TFA (7). This compound was prepared starting from 2,3-benzoic acid and aminomalononitrile via intermediate **7i** following the above general procedure. LC-MS retention time: (method 3) 2.639 and (method 2) = 3.559 min. ^{1}H NMR (400 MHz, DMSO-d_6) δ 8.50 (q, J = 4.9 Hz, 1H), 7.83 (ddd, J = 7.9, 1.5, 0.4 Hz, 1H), 7.78 (ddd, J = 8.1, 1.6, 0.4 Hz, 1H), 7.54–7.46 (m, 1H), 2.99 (d, J = 4.9 Hz, 3H). HRMS (ESI): m/z (M + H)$^+$ calcd for C$_{11}$H$_8$Cl$_2$N$_3$O, 269.0039; found, 269.0031.

2-(3,4-Dichlorophenyl)-5-(methylamino)oxazole-4-carbonitrile TFA (8). This compound was prepared starting from 3,4-benzoic acid and aminomalononitrile via intermediate **8i** following the above general procedure. LC-MS retention time: (method 2) 3.737 min. ^{1}H NMR (400 MHz, DMSO-d_6) δ 8.48 (q, J = 4.9 Hz, 1H), 7.95 (td, J = 1.8, 0.7 Hz, 1H), 7.80–7.72 (m, 2H), 3.09–2.91 (m, 3H). HRMS (ESI): m/z (M + H)$^+$ calcd for C$_{11}$H$_8$Cl$_2$N$_3$O, 269.0039; found, 269.0043.

2-([1,1′-Biphenyl]-4-yl)-5-(methylamino)oxazole-4-carbonitrile TFA (11). This compound was prepared starting from 4-phenylbenzoic

acid and aminomalononitrile via intermediate **11i** following the above general procedure. LC-MS retention time: (method 1) 6.215 and (method 2) 3.708 min, ^{1}H NMR (400 MHz, DMSO-d_6) δ 8.38 (q, J = 4.9 Hz, 1H), 7.92−7.79 (m, 4H), 7.76−7.68 (m, 2H), 7.53−7.46 (m, 2H), 7.43−7.37 (m, 1H), 3.01 (dd, J = 4.8, 0.6 Hz, 3H). HRMS (ESI): m/z (M + H)$^+$ calcd for $C_{17}H_{14}N_3O$, 276.1131; found, 276.1143.

Synthesis of 5-(azetidin-3-ylamino)-2-(naphthalen-1-yl)oxazole-4-carbonitrile TFA (31). A mixture of 5-chloro-2-(naphthalen-1-yl)oxazole-4-carbonitrile (**19a**) (details of the synthesis are provided in the Supporting Information) (0.25 mmol, 1 equiv) and 1-boc-3-(amino)azetidine (1 mmol, 4 equiv) in THF was heated to reflux for 0.5 h. The reaction mixture was then cooled, and the solvent was removed by forced air. The crude product was taken up in DMSO and purified via reversed-phase preparative HPLC. This pure product was suspended in dichloromethane (2 mL) and treated with TFA (0.5 mL). After stirring for 0.5 h at room temperature, the volatiles were removed by forced air. The crude product was taken up in DMSO and purified on a preparative HPLC to give pure product (**31**) as its TFA salt. LC-MS retention time: (method 1) 4.078 and (method 2) 3.812 min, ^{1}H NMR (400 MHz, DMSO-d_6) δ 9.29 (s, 1H), 9.12 (d, J = 8.6 Hz, 1H), 8.90 (s, 1H), 8.14−8.01 (m, 2H), 7.75−7.59 (m, 3H), 4.77 (p, J = 7.0, 6.0 Hz, 1H), 4.32−4.18 (m, 2H), 4.18−4.08 (m, 2H), HRMS (ESI): m/z (M + H)$^+$ calcd for $C_{17}H_{15}N_4O$, 291.1252; found, 291.125.

Synthesis of (methylamino)-2-(naphthalen-1-yl)thiazole-4-carbonitrile TFA (32). A mixture of 2-bromothiazole-4-carbonitrile (1.85 g, 9.79 mmol, 1 equiv), naphthalen-1-ylboronic acid (2.52 g, 14.68 mmol, 1.5 equiv), 2 M sodium carbonate (12.23 mL, 24.47 mmol, 2.5 equiv), and Pd(PPh$_3$)$_4$ (1.11 g, 0.979 mmol, 10 mol %) in dimethoxy ethane (20 mL) was degassed with argon and then heated under microwave for 45 min at 150 °C. The reaction mixture was concentrated, taken up in dichloromethane, stirred with palladium scavenger resin, and filtered through Celite. The crude product obtained after evaporating the solvent was purified on a biotage flash system, eluting with 10% ethyl acetate in hexanes to obtain 1.52 g (yield: 66%) of 2-(naphthalen-1-yl)thiazole-4-carbonitrile (**32a**) as a white solid.

A solution of the above 2-(naphthalen-1-yl)thiazole-4-carbonitrile **32a** (0.5 g, 2.12 mmol, 1 equiv) in THF (10 mL) was added a 2 M THF solution of LDA (1.16 mL, 2.33 mmol, 1.1 equiv) dropwise at −78 °C. After stirring for 30 min at −78 °C, perchloroethane (0.551 g, 2.33 mmol, 1.1 equiv) was added in one portion and allowed to warm to room temperature over 4 h. The reaction was then quenched with saturated ammonium chloride and extracted with ethyl acetate. The organic layer was washed with water and brine. The ethyl acetate layer was subsequently dried over MgSO$_4$ and filtered. The crude product obtained after concentrating under diminished pressure was purified on a Biotage flash system, eluting with 50% CH$_2$Cl$_2$ in hexanes to furnish 4.5 g (yield: 79%) of 5-chloro-2-(naphthalen-1-yl)thiazole-4-carbonitrile **32b** as a white solid. ^{1}H NMR (400 MHz, DMSO-d_6) δ 8.67 (d, J = 8.4 Hz, 1H), 8.20 (d, J = 8.3 Hz, 1H), 8.13−8.05 (m, 1H), 7.94 (dd, J = 7.3, 1.3 Hz, 1H), 7.69 (dddd, J = 14.7, 9.3, 6.9, 1.7 Hz, 3H).

A mixture of 5-chloro-2-(naphthalen-1-yl)thiazole-4-carbonitrile **32b** (0.2 g, 0.739 mmol, 1 equiv) and a 2 M THF solution of methylamine (1.9 mL, 3.69 mmol, 5 equiv) in 2-propanol (1 mL) was heated via microwave for 30 min at 120 °C. The crude product obtained after evaporation of the solvent was taken up in DMSO and purified by reversed-phase preparative HPLC to obtain 5-(methyl-amino)-2-(naphthalen-1-yl)thiazole-4-carbonitrile (**32**) as its TFA salt. LC-MS retention time: (method 3) 2.814 and (method 2) 3.756 min, ^{1}H NMR (400 MHz, DMSO-d_6) δ 8.88 (ddt, J = 8.5, 1.4, 0.8 Hz, 1H), 8.17 (q, J = 4.7 Hz, 1H), 8.07−7.98 (m, 2H), 7.77 (dd, J = 7.2, 1.2 Hz, 1H), 7.71−7.53 (m, 3H), 3.01 (d, J = 4.7 Hz, 3H), HRMS (ESI): m/z (M + H)$^+$ calcd for $C_{15}H_{12}N_3S$, 266.0754; found, 266.0746.

Synthesis of N-methyl-5-(naphthalen-1-yl)oxazol-2-amine (34). A solution of 5-(naphthalen-1-yl)oxazole-4-carbonitrile **34a** (0.9 g, 4.09 mmol, 1 equiv) in THF (15 mL) was added a 1 M THF solution of LHMDS (4.5 mL, 4.5 mmol, 1.1 equiv) dropwise at −78 °C. The reaction mixture was stirred for 30 min at −78 °C, perchloroethane

(1.064 g, 4.5 mmol, 1.1 equiv) was added in one portion, and the mixture was allowed to reach room temperature over 4 h. The reaction mixture was quenched with saturated ammonium chloride and extracted with ethyl acetate. The organic layer was washed with water and brine, dried over magnesium sulfate, filtered, and concentrated under diminished pressure. The crude product was purified on a Biotage flash system, eluting with 10% ethyl acetate in hexanes to furnish 0.75 g (yield: 72%) of 2-chloro-5-(naphthalen-1-yl)oxazole-4-carbonitrile **34b** as a white solid.

A solution of 2-chloro-5-(naphthalen-1-yl)oxazole-4-carbonitrile **34b** (0.1 g, 0.393 mmol, 1 equiv) in THF (1 mL) was added a 2 M solution of methanamine in THF (1.0 mL, 1.98 mmol, 5 equiv) and stirred at 65 °C for 1 h in a sealed tube. The solvent was removed by forced air to obtain a crude solid. This crude product was taken up in DMSO and purified on a preparative HPLC to obtain pure product (**34**) as its TFA salt. LC-MS retention time: (method 1) 5.509 and (method 2) 3.498 min, ^{1}H NMR (400 MHz, DMSO-d_6) δ 8.17−7.96 (m, 4H), 7.81 (dd, J = 7.3, 1.3 Hz, 1H), 7.71−7.59 (m, 3H), 2.88 (d, J = 4.8 Hz, 3H), HRMS (ESI): m/z (M + H)$^+$ calcd for $C_{15}H_{12}N_3O$, 250.0975; found, 250.0979.

Materials and Methods. *Materials.* Different commercial fatty acids as lipoxygenase substrates, were purchased from Nu Chek Prep, Inc. (MN, USA). The fatty acids were further repurified using a Higgins HAISIL (5 μm, 250 × 10 mm) C-18 column. An isocratic elution of 85% solvent A (99.9% methanol and 0.1% acetic acid)/15% solvent B (99.9% water and 0.1% acetic acid) was used to purify all the fatty acids. Post purification, the fatty acids were stored at −80 °C for a maximum of 6 months. Lipoxygenase product 13-(S)-HPODE was generated by reacting LA with soybean LOX-1. The product generation protocol involved reacting 50 μM substrate in 500 mL of 100 mM borate buffer, pH 9.2, with soybean LOX-1. A small sample from the larger reaction was monitored on the UV−vis spectrometer until complete turnover was observed. The products were then extracted using dichloromethane, reduced with trimethylphosphite, evaporated to dryness, and reconstituted in methanol. The products were HPLC-purified using an isocratic elution of 75% A (99.9% methanol and 0.1% acetic acid)/25% B (99.9% water and 0.1% acetic acid). The products were tested for their purity using LC−MS/MS and were found to be >98% pure. Ovine COX-1 (catalog no. 60100) and human COX-2 (catalog no. 60122) were purchased from Cayman chemicals. All other chemicals were of high quality and used without further purification.

High-Throughput Screen. See Supporting Information.

Overexpression and Purification of Lipoxygenases. Different lipoxygenases, such as human reticulocyte 15-lipoxygenase-1 (12/15-LOX), human epithelial 15-lipoxygenase-2 (15-LOX-2), and human platelet 12-lipoxygenase (12-LOX), were expressed as N-terminal His$_6$-tagged proteins and were purified via immobilized metal-affinity chromatography using Ni-NTA resins for 12/15-LOX and 15-LOX-2, whereas Ni-IDA resin was used for 12-LOX.[75,76] The protein purity was evaluated by SDS-PAGE analysis and was found to be greater than 90%. Human 5-lipoxygenase (5-LOX) was expressed as a nontagged protein and used as a crude ammonium sulfate protein fraction, as published previously.[77]

Lipoxygenase UV−Vis Assay. The inhibitor compounds were screened initially using one concentration point on a PerkinElmer Lambda 40 UV−vis spectrometer. The percent inhibition was determined by comparing the enzyme rates of the control (DMSO solvent) and the inhibitor sample by following the formation of the conjugated diene product at 234 nm (ε = 25 000 M^{-1} cm^{-1}). The reactions were initiated by adding either ∼40 nM 12-LOX, 40 nM 12/15-LOX, 0.5 μM 15-LOX-2, or ∼200 nM 5-LOX (ammonium sulfate suspension) to a cuvette with a 2 mL of reaction buffer that was constantly stirred using a magnetic stirrer bar at room temperature (22 °C). It should be noted that LOX isozymes are often expressed in the inactive demetalated form, so it is best to utilize activity to determine the optimal LOX concentration for the assay (optimal rate of approximately 0.001 abs/s at 10 μM AA). Reaction buffers used for various lipoxygenase were as follows: 25 mM HEPES (pH 7.3), 0.3 mM CaCl$_2$, 0.1 mM EDTA, 0.2 mM ATP, 0.01% Triton X-100, and 10

μM AA for the crude, ammonium sulfate-precipitated 5-LOX; 25 mM Hepes (pH 8), 0.01% Triton X-100, and 10 μM AA for 12-LOX, and 25 mM Hepes buffer (pH 7.5), 0.01% Triton X-100, and 10 μM AA for 12/15-LOX and 15-LOX-2. The substrate concentration was quantitatively determined by allowing the enzymatic reaction to go to completion in the presence of 15-LOX-2. For the inhibitors that showed more than 50% inhibition at the one-point screens (25 μM inhibitor), IC_{50} values were obtained by determining the enzymatic rate at various inhibitor concentrations and were plotted against inhibitor concentration (approximate range: 0.1−25 μM inhibitor) followed by a hyperbolic saturation curve fit (assuming total enzyme concentration $[E] \ll K_i^{app}$, so $IC_{50} \sim K_i^{app}$). It should be noted that all of the potent inhibitors displayed greater than 80% maximal inhibition unless it is otherwise stated in the tables. Inhibitors were stored at −20 °C in DMSO.

Pseudoperoxidase Assay. The pseudoperoxidase activity rates were determined with BWb70c as the positive control, 13-(S)-HPODE as the oxidizing product. and 12/15-LOX on a PerkinElmer Lambda 40 UV−vis spectrometer, as described previously.[78] Briefly, activity was determined by monitoring the decrease at 234 nm (product degradation) in buffer (50 mM sodium phosphate (pH 7.4), 0.3 mM $CaCl_2$, 0.1 mM EDTA, 0.01% Triton X100, and 20 μM 13-(S)-HPODE). 12/15-LOX was added to buffer (22 °C), and the reaction initiated by addition of 20 μM inhibitor (1:1 ratio to product). The percent consumption of 13-(S)-HPODE was recorded, with individual controls being conducted with inhibitor alone with product and enzyme alone with product.

Steady-State Inhibition Kinetics. The steady-state kinetics experiments were performed with the parent analogue, compound **1** (**ML351**), to determine the mode of inhibition, as described previously.[56,79] The inhibitor concentrations of 0, 0.05, 2, and 5 μM were used. Reactions were initiated by adding approximately 40−60 nM 12/15-LOX to a constantly stirring 2 mL cuvette containing 1−20 μM AA in 25 mM HEPES buffer (pH 7.5) in the presence of 0.01% Triton X-100. Lipoxygenase rates were determined by monitoring the formation of the conjugated product, 15-HpETE, at 234 nm ($\varepsilon = 25\,000$ M^{-1} cm^{-1}) with a PerkinElmer Lambda 40 UV−vis spectrometer. The substrate concentration was quantitatively determined by allowing the enzymatic reaction to proceed to completion using 15-LOX-2. Kinetic data were obtained by recording initial enzymatic rates at varied substrate and inhibitor concentrations, and the data were subsequently fitted to the Henri−Michaelis−Menten equation using KaleidaGraph (Synergy) to determine the microscopic rate constants, V_{max} (μmol/min/mg) and V_{max}/K_m (μmol/min/mg/μM). These rate constants were subsequently replotted with $1/V_{max}$ and K_m/V_{max} versus inhibitor concentration, yielding K_i' and K_i, respectively.

Cyclooxygenase Assay. About 2−5 μg of either COX-1 or COX-2 were added to buffer containing 0.1 M Tris-HCl buffer (pH 8.0), 5 mM EDTA, 2 mM phenol, and 1 μM hematin at 37 °C. The inhibitors were added to the reaction cell followed by an incubation of 5 min with either of the COX enzymes. The reaction was then initiated by adding 100 μM AA in the reaction cell. Data was collected using a Hansatech DW1 oxygen electrode, and the consumption of oxygen was recorded. Indomethacin and the solvent, DMSO, were used as positive and negative controls, respectively, and the percent inhibition of the enzyme was calculated by comparing the rates from samples and the controls.

HT22 Cell Culture Assay. Glutathione depletion was induced in HT22 cells by glutamate treatment, and LDH release into the medium was measured to detect cell death, as described previously.[38] Briefly, HT22 cells were cultured in DMEM containing 10% fetal bovine serum and penicillin/streptomycin (all media from Invitrogen). For viability experiments, cells were seeded at 1×10^4 cells/well in 96-well plates (Corning) and were treated 18 h later when the cells were approximately 50−70% confluent. Treatment consisted of exchanging the medium to 100 μL of fresh culturing medium and adding 5 mM glutamate (stock solution 0.5 M in PBS) in the presence or absence of DMSO (maximum 0.1% final concentration) as control or the indicated concentrations of **1**. LDH content was determined separately for the cell extracts and corresponding media using a Cytotoxicity

Detection Kit (Roche), and the percentage of LDH released to the medium was calculated after subtracting the corresponding background value. To determine levels of the 12/15-LOX metabolite, 12-HETE, we cultured HT22 cells in 75 cm^2 flasks in DMEM medium without phenol red that was supplemented with 5% FBS, and the cells were treated the next day when they were 50−70% confluent. Twenty-four hours later, the eicosanoid-containing fraction was isolated via Sep-Pak C-18 column, and 12-HETE was detected with a 12-HETE ELISA kit (Enzo Life Sciences), which was used according to the manufacturer's instructions. Three independent experiments were evaluated. For the MS samples, the above procedure was modified slightly. The eicosanoids containing fractions were transferred to scintillation vials followed by addition of perdeuterated 13-HODE (13-d_{31}-HODE) as an internal control for extraction and 1.5% glacial acetic acid for protein precipitation. The samples were extracted with methylene chloride, reduced with trimethylphosphite, and evaporated to dryness. The dry samples were then reconstituted in methanol, and an internal control 12-deuterated (d_8)-HETE (12-d_8-HETE) was added to each sample for detector response variation; it was assumed that the change in detector response for 12-HETE and 12-d_8-HETE would be similar. The samples were run on and analyzed by a Finnigan LTQ liquid chromatography−tandem mass spectrometry (LC−MS/MS) system. A Thermo Electron Corp. Aquasil (3 μm, 100 mm × 2.1 mm) C-18 column was used to detect the HETEs with an elution protocol consisting of a 0.2 mL/min flow rate and a linear gradient from 54.9% ACN, 45% H_2O, and 0.1% THF to 69.9% ACN, 30% H_2O, and 0.1% THF. The electrospray voltage was set to 5.0 kV and a global acquisition MS mode was used. The MS−MS scan was performed for the five most abundant precursor ions. The collision-induced dissociation was used for MS−MS with a collision energy of 35 eV. The corresponding 12-HETE, 12-d_8-HETE, and 13-d_{31}-HODE compounds were detected using selective ion monitoring analysis (m/z = 318.7−319.7, 326.8−327.7, and 325.8−326.8, respectively) in negative ion mode and then identified by fragmentation pattern (12-HETE, parent ion at m/z 319 and fragments at m/z 179 and 163; 12-d_8-HETE, parent ion at m/z 327 and fragments at m/z 184; and 13-d_{31}-HODE, parent ion m/z 326 and fragments at m/z 213) from MS−MS. The peak area of 12-d_8-HETE for each sample was normalized to the area of 13-d_{31}-HODE. The peak intensities of 12-HETEs were normalized to the corrected 12-d_8-HETE intensities. The amount of 12-HETE in samples was estimated from the pure 12-(S)-HETE standard curve.

Distal MCAO Model of Permanent Focal Ischemia in Mice. To study **1** in a model of distal MCAO,[74] C57Bl6J mice were treated with ferric chloride ($FeCl_3$) to cause occlusion of the distal middle cerebral artery. Mice were kept under anesthesia with 1.5% isoflurane in a nitrous oxide/oxygen mixture via facemask. The body temperature was monitored by a rectal probe and maintained at 37 ± 0.3 °C by a homeothermic blanket control unit. Briefly, mice were placed in a stereotaxic frame, the scalp was opened, and the right temporal muscle was dissected. The area between zygomatic arch and squamous bone was thinned by a high-speed drill and cooled with saline. The trace of MCA was visualized, and the thin bony film was lifted up by forceps. After that, a laser doppler flowmetry probe was placed 2 mm posterior and 6 mm lateral to the bregma to monitor the regional cerebral blood flow (rCBF). After obtaining a stable epoch of the preischemic rCBF, a piece of 10% $FeCl_3$-saturated filter paper was placed over the intact dura mater along the trace of MCA, and the rCBF was continuously monitored during the next 3 h. After 2 h of ischemia, either 50 mg/kg of **1** or DMSO vehicle was injected intraperitoneally. Following sacrifice at 24 h, brains were sectioned into 1 mm slices, and infarct sizes were determined by staining with TTC using the indirect method (infarct volume = contralateral volume minus uninfarcted ipsilateral volume). Both the surgeon carrying out the procedure and the researcher determining infarct volumes were blinded as to which treatment the mice received.

ASSOCIATED CONTENT

Supporting Information

Additional experimental procedures; spectroscopic (^{1}H), LC/MS, and HRMS data for representative compounds; and qHTS assay performance. This material is available free of charge via the Internet at http://pubs.acs.org.

AUTHOR INFORMATION

Corresponding Authors

*(K.v.L.) Tel: 617-724-6556; Fax: 617-726-7830; E-mail: klaus_vanleyen@hms.harvard.edu.
*(D.J.M.) Tel: 301-217-4381; Fax: 301-217-5736; E-mail: maloneyd@mail.nih.gov.
*(T.R.H.) Tel: 831-459-5884; Fax: 831-459-2935; E-mail: tholman@chemistry.ucsc.edu.

Author Contributions

‖G.R., N.J., J.E.J, and Y.L. contributed equally to this work.

Notes

The authors declare no competing financial interest.

ACKNOWLEDGMENTS

ABBREVIATIONS USED

LOX, lipoxygenase; sLOX-1, soybean lipoxygenase-1; 12/15-LOX, human reticulocyte 15-lipoxygenase-1; 15-LOX-1, human reticulocyte 15-lipoxygenase-1; 15-LOX-2, human epithelial 15-lipoxygenase-2; 12-LOX, human platelet 12-lipoxygenase; rabbit 12/15-LOX, rabbit reticulocyte 12/15-lipoxygenase; mouse 12/15-LOX, mouse reticulocyte 12/15-lipoxygenase; COX, cyclooxygenase; NDGA, nordihydroguaiaretic acid; AA, arachidonic acid; 15-HpETE, 15-(S)-hydroperoxyeicosatetraenoic acid; 12-HpETE, 12-(S)-hydroperoxyeicosatetraenoic acid; LA, linoleic acid; 13-(S)-HpODE, 13-(S)-hydroperoxyoctadecadienoic acid; 12-HETE, 12-(S)-hydroxyeicosatetraenoic acid; 15-HETE, 15-(S)-hydroxyeicosatetraenoic acid; V_{max}, maximal velocity (μmol/min); K_m, Henri−Michaelis−Menten Constant (μM); [E], total active enzyme concentration; IC$_{50}$, inhibitor constant at 50% inhibition; K_i^{app}, apparent inhibition constant when [E] $\gg K_i^{app}$; XO, xylenol orange; HTS, high-throughput screening; MLSMR, Molecular Libraries Small Molecule Repository; MLPCN, Molecular Libraries Probe Centers Network; qHTS, quantitative high-throughput screening; CRC, concentration response curve; EDC, 1-ethyl-3-(3-(dimethylamino)propyl)carbodiimide hydrochloride; BTAC, *N*-benzyl-triethylammonium chloride; BWB70C, *N*-[3-[3-(fluorophenoxy)phenyl]-1-methyl-2-propenyl]-*N*-hydroxyurea; LDA, lithium diisopropylamide

REFERENCES

(1) Solomon, E. I.; Zhou, J.; Neese, F.; Pavel, E. G. New Insights from Spectroscopy into the Structure/Function Relationships of Lipoxygenases. *Chem. Biol.* **1997**, *4*, 795−808.

(2) Brash, A. R. Lipoxygenases: Occurrence, Functions, Catalysis and Acquisition of Substrate. *J. Biol. Chem.* **1999**, *274*, 23679−23682.

(3) Ivanov, I.; Heydeck, D.; Hofheinz, K.; Roffeis, J.; O'Donnell, V. B.; Kuhn, H.; Walther, M. Molecular Enzymology of Lipoxygenases. *Arch. Biochem. Biophys.* **2010**, *503*, 161−174.

(4) Schnurr, K.; Belkner, J.; Ursini, F.; Schewe, T.; Kuhn, H. The Selenoenzyme Phospholipid Hydroperoxide Glutathione Peroxidase Controls the Activity of the 15-Lipoxygenase with Complex Substrates and Preserves the Specificity of the Oxygenation Products. *J. Biol. Chem.* **1996**, *271*, 4653−4658.

(5) Tong, W. G.; Ding, X. Z.; Hennig, R.; Witt, R. C.; Standop, J.; Pour, P. M.; Adrian, T. E. Leukotriene B4 Receptor Antagonist LY293111 Inhibits Proliferation and Induces Apoptosis in Human Pancreatic Cancer Cells. *Clin. Cancer Res.* **2002**, *8*, 3232−3242.

(6) Wenzel, S. E.; Kamada, A. K. Zileuton: The First 5-Lipoxygenase Inhibitor for the Treatment of Asthma. *Ann. Pharmacother.* **1996**, *30*, 858−864.

(7) O'Byrne, P. M.; Israel, E.; Drazen, J. M. Antileukotrienes in the Treatment of Asthma. *Ann. Int. Med.* **1997**, *127*, 472−480.

(8) Berger, W.; De Chandt, M. T.; Cairns, C. B. Zileuton: Clinical Implications of 5-Lipoxygenase Inhibition in Severe Airway Disease. *Int. J. Clin. Pract.* **2007**, *61*, 663−6676.

(9) Muller-Peddinghaus, R. Potential Anti-Inflammatory Effects of 5-Lipoxygenase Inhibition−Exemplified by the Leukotriene Synthesis Inhibitor BAY X 1005. *J. Physiol. Pharmacol.* **1997**, *48*, 529−536.

(10) Klickstein, L. B.; Shapleigh, C.; Goetzl, E. J. Lipoxygenation of Arachidonic Acid as a Source of Polymorphonuclear Leukocyte Chemotactic Factors in Synovial Fluid and Tissue in Rheumatoid Arthritis and Spondyloarthritis. *J. Clin. Invest.* **1980**, *66*, 1166−1170.

(11) Weinblatt, M. E.; Kremer, J. M.; Coblyn, J. S.; Helfgott, S.; Maier, A. L.; Petrillo, G.; Henson, B.; Rubin, P.; Sperling, R. Zileuton, a 5-Lipoxygenase Inhibitor in Rheumatoid Arthritis. *J. Rheumatol.* **1992**, *19*, 1537−1541.

(12) Spanbroek, R.; Grabner, R.; Lotzer, K.; Hildner, M.; Urbach, A.; Ruhling, K.; Moos, M. P.; Kaiser, B.; Cohnert, T. U.; Wahlers, T.; Zieske, A.; Plenz, G.; Robenek, H.; Salbach, P.; Kuhn, H.; Radmark, O.; Samuelsson, B.; Habenicht, A. J. Expanding Expression of the 5-Lipoxygenase Pathway within the Arterial Wall During Human Atherogenesis. *Proc. Natl. Acad. Sci. U.S.A.* **2003**, *100*, 1238−1243.

(13) Funk, C. D. Leukotriene Modifiers as Potential Therapeutics for Cardiovascular Disease. *Nat. Rev. Drug Discovery* **2005**, *4*, 664−6672.

(14) Lotzer, K.; Funk, C. D.; Habenicht, A. J. The 5-Lipoxygenase Pathway in Arterial Wall Biology and Atherosclerosis. *Biochim. Biophys. Acta* **2005**, *1736*, 30−37.

(15) Bleich, D.; Chen, S.; Gu, J. L.; Nadler, J. L. The Role of 12-Lipoxygenase in Pancreatic Cells (Review). *Int. J. Mol. Med.* **1998**, *1*, 265−272.

(16) Hedrick, C. C.; Kim, M. D.; Natarajan, R. D.; Nadler, J. L. 12-Lipoxygenase Products Increase Monocyte:Endothelial Interactions. *Adv. Exp. Med. Biol.* **1999**, *469*, 455−460.

(17) Thomas, C. P.; Morgan, L. T.; Maskrey, B. H.; Murphy, R. C.; Kuhn, H.; Hazen, S. L.; Goodall, A. H.; Hamali, H. A.; Collins, P. W.; O'Donnell, V. B. Phospholipid-Esterified Eicosanoids Are Generated in Agonist-Activated Human Platelets and Enhance Tissue Factor-Dependent Thrombin Generation. *J. Biol. Chem.* **2010**, *285*, 6891−6903.

(18) Hussain, H.; Shornick, L. P.; Shannon, V. R.; Wilson, J. D.; Funk, C. D.; Pentland, A. P.; Holtzman, M. J. Epidermis Contains Platlet-Type 12-Lipoxygenase That Is Overexpressed in Germinal

Layer Keratinocytes in Psoriasis. *Am. J. Physiol.* **1994**, *266*, C243−C253.

(19) Connolly, J. M.; Rose, D. P. Enhanced Angiogenesis and Growth of 12-Lipoxygenase Gene-Transfected MCF-7 Human Breast Cancer Cells in Athymic Nude Mice. *Cancer Lett.* **1998**, *132*, 107−112.

(20) Ding, X. Z.; Iversen, P.; Cluck, M. W.; Knezetic, J. A.; Adrian, T. E. Lipoxygenase Inhibitors Abolish Proliferation of Human Pancreatic Cancer Cells. *Biochem. Biophys. Res. Commun.* **1999**, *261*, 218−223.

(21) Haeggstrom, J.; Funk, C. D. Lipoxygenase and Leukotriene Pathways: Biochemistry, Biology, and Roles in Disease. *Chem. Rev.* **2011**, *111*, 5866−5898.

(22) Kuhn, H.; Walther, M.; Kuban, R. J. Mammalian Arachidonate 15-Lipoxygenases: Structure, Function, and Biological Implications. *Prostaglandins Other Lipid Mediators* **2002**, *68−69*, 263−290.

(23) Weaver, J. R.; Holman, T. R.; Imai, Y.; Jadhav, A.; Kenyon, V.; Maloney, D. J.; Nadler, J. L.; Rai, G.; Simeonov, A.; Taylor-Fishwick, D. A. Integration of Pro-Inflammatory Cytokines, 12-Lipoxygenase and Nox-1 in Pancreatic Islet Beta Cell Dysfunction. *Mol. Cell. Endocrinol.* **2012**, *358*, 88−95.

(24) Stavniichuk, R.; Drel, V. R.; Shevalye, H.; Vareniuk, I.; Stevens, M. J.; Nadler, J. L.; Obrosova, I. G. Role of 12/15-Lipoxygenase in Nitrosative Stress and Peripheral Prediabetic and Diabetic Neuropathies. *Free Radical Biol. Med.* **2010**, *49*, 1036−1045.

(25) Obrosova, I. G.; Stavniichuk, R.; Drel, V. R.; Shevalye, H.; Vareniuk, I.; Nadler, J. L.; Schmidt, R. E. Different Roles of 12/15-Lipoxygenase in Diabetic Large and Small Fiber Peripheral and Autonomic Neuropathies. *Am. J. Pathol.* **2010**, *177*, 1436−1447.

(26) Dobrian, A. D.; Lieb, D. C.; Ma, Q.; Lindsay, J. W.; Cole, B. K.; Ma, K.; Chakrabarti, S. K.; Kuhn, N. S.; Wohlgemuth, S. D.; Fontana, M.; Nadler, J. L. Differential Expression and Localization of 12/15 Lipoxygenases in Adipose Tissue in Human Obese Subjects. *Biochem. Biophys. Res. Commun.* **2010**, *403*, 485−490.

(27) Chakrabarti, S. K.; Wen, Y.; Dobrian, A. D.; Cole, B. K.; Ma, Q.; Pei, H.; Williams, M. D.; Bevard, M. H.; Vandenhoff, G. E.; Keller, S. R.; Gu, J.; Nadler, J. L. Evidence for Activation of Inflammatory Lipoxygenase Pathways in Visceral Adipose Tissue of Obese Zucker Rats. *Am. J. Physiol.: Endocrinol. Metab.* **2010**, *300*, E175−E187.

(28) Nunemaker, C. S.; Chen, M.; Pei, H.; Kimble, S. D.; Keller, S. R.; Carter, J. D.; Yang, Z.; Smith, K. M.; Wu, R.; Bevard, M. H.; Garmey, J. C.; Nadler, J. L. 12-Lipoxygenase-Knockout Mice Are Resistant to Inflammatory Effects of Obesity Induced by Western Diet. *Am. J. Physiol.: Endocrinol. Metab.* **2008**, *295*, E1065−E1075.

(29) Succol, F.; Pratico, D. A Role for 12/15 Lipoxygenase in the Amyloid Beta Precursor Protein Metabolism. *J. Neurochem.* **2007**, *103*, 380−387.

(30) Yao, Y.; Clark, C. M.; Trojanowski, J. Q.; Lee, V. M.; Pratico, D. Elevation of 12/15 Lipoxygenase Products in AD and Mild Cognitive Impairment. *Ann. Neurol.* **2005**, *58*, 623−626.

(31) Pratico, D.; Zhukareva, V.; Yao, Y.; Uryu, K.; Funk, C. D.; Lawson, J. A.; Trojanowski, J. Q.; Lee, V. M. 12/15-Lipoxygenase Is Increased in Alzheimer's Disease: Possible Involvement in Brain Oxidative Stress. *Am. J. Pathol.* **2004**, *164*, 1655−1662.

(32) Haynes, R. L.; van Leyen, K. 12/15-Lipoxygenase Expression Is Increased in Oligodendrocytes and Microglia of Periventricular Leukomalacia. *Dev. Neurobiol.* **2013**, *35*, 140−154.

(33) O'Flaherty, J. T.; Wooten, R. E.; Samuel, M. P.; Thomas, M. J.; Levine, E. A.; Case, L. D.; Akman, S. A.; Edwards, I. J. Fatty Acid Metabolites in Rapidly Proliferating Breast Cancer. *PLoS One* **2013**, *8*, e63076-1−e63076-8.

(34) Yigitkanli, K.; Pekcec, A.; Karatas, H.; Pallast, S.; Mandeville, E.; Joshi, N.; Smirnova, N.; Gazaryan, I.; Ratan, R. R.; Witztum, J. L.; Montaner, J.; Holman, T. R.; Lo, E. H.; van Leyen, K. Inhibition of 12/15-Lipoxygenase as Therapeutic Strategy to Treat Stroke. *Ann. Neurol.* **2013**, *73*, 129−135.

(35) van Leyen, K. Lipoxygenase: An Emerging Target for Stroke Therapy. *CNS Neurol. Disord.: Drug Targets* **2013**, *12*, 191−199.

(36) Lo, E. H.; Dalkara, T.; Moskowitz, M. A. Mechanisms, Challenges and Opportunities in Stroke. *Nat. Rev. Neurosci.* **2003**, *4*, 399−415.

(37) Donnan, G. A.; Fisher, M.; Macleod, M.; Davis, S. M. Stroke. *Lancet.* **2008**, *371*, 1612−1623.

(38) Li, Y.; Maher, P.; Schubert, D. A Role for 12-Lipoxygenase in Nerve Cell Death Caused by Glutathione Depletion. *Neuron* **1997**, *19*, 453−463.

(39) Lovat, P. E.; Oliverio, S.; Ranalli, M.; Corazzari, M.; Rodolfo, C.; Bernassola, F.; Aughton, K.; Maccarrone, M.; Hewson, Q. D.; Pearson, A. D.; Melino, G.; Piacentini, M.; Redfern, C. P. Gadd153 and 12-Lipoxygenase Mediate Fenretinide-Induced Apoptosis of Neuroblastoma. *Cancer Res.* **2002**, *62*, 5158−5167.

(40) Canals, S.; Casarejos, M. J.; de Bernardo, S.; Rodriguez-Martin, E.; Mena, M. A. Nitric Oxide Triggers the Toxicity Due to Glutathione Depletion in Midbrain Cultures through 12-Lipoxygenase. *J. Biol. Chem.* **2003**, *278*, 21542−21549.

(41) Khanna, S.; Roy, S.; Ryu, H.; Bahadduri, P.; Swaan, P. W.; Ratan, R. R.; Sen, C. K. Molecular Basis of Vitamin E Action: Tocotrienol Modulates 12-Lipoxygenase, a Key Mediator of Glutamate-Induced Neurodegeneration. *J. Biol. Chem.* **2003**, *278*, 43508−43515.

(42) Khanna, S.; Roy, S.; Slivka, A.; Craft, T. K.; Chaki, S.; Rink, C.; Notestine, M. A.; DeVries, A. C.; Parinandi, N. L.; Sen, C. K. Neuroprotective Properties of the Natural Vitamin E Alpha-Tocotrienol. *Stroke* **2005**, *36*, 2258−2264.

(43) van Leyen, K.; Kim, H. Y.; Lee, S. R.; Jin, G.; Arai, K.; Lo, E. H. Baicalein and 12/15-Lipoxygenase in the Ischemic Brain. *Stroke* **2006**, *37*, 3014−3018.

(44) van Leyen, K.; Lee, S. R.; Siddiq, A.; Ratan, R. R.; Lo, E. H. 12/15-Lipoxygenase and the Proteasome as Mediators of Neuronal Oxidative Stress and Stroke, Program No. 1356, Society for Neuroscience 34th Annual Meeting, San Diego, CA, Oct 23−27, 2004; Society for Neuroscience: Washington, DC, 2004.

(45) Jin, G.; Arai, K.; Murata, Y.; Wang, S.; Stins, M. F.; Lo, E. H.; van Leyen, K. Protecting against Cerebrovascular Injury: Contributions of 12/15-Lipoxygenase to Edema Formation Following Transient Focal Ischemia. *Stroke* **2008**, *39*, 2538−2543.

(46) Pallast, S.; Arai, K.; Wang, X.; Lo, E. H.; van Leyen, K. 12/15-Lipoxygenase Targets Neuronal Mitochondria under Oxidative Stress. *J. Neurochem.* **2009**, *111*, 882−889.

(47) Pallast, S.; Arai, K.; Pekcec, A.; Yigitkanli, K.; Yu, Z.; Wang, X.; Lo, E. H.; van Leyen, K. Increased Nuclear Apoptosis-Inducing Factor after Transient Focal Ischemia: A 12/15-Lipoxygenase-Dependent Organelle Damage Pathway. *J. Cereb. Blood Flow Metab.* **2010**, *30*, 1157−1167.

(48) Seiler, A.; Schneider, M.; Forster, H.; Roth, S.; Wirth, E. K.; Culmsee, C.; Plesnila, N.; Kremmer, E.; Radmark, O.; Wurst, W.; Bornkamm, G. W.; Schweizer, U.; Conrad, M. Glutathione Peroxidase 4 Senses and Translates Oxidative Stress into 12/15-Lipoxygenase Dependent- and AIF-Mediated Cell Death. *Cell Metab.* **2008**, *8*, 237−248.

(49) Kenyon, V.; Chorny, I.; Carvajal, W. J.; Holman, T. R.; Jacobson, M. P. Novel Human Lipoxygenase Inhibitors Discovered Using Virtual Screening with Homology Models. *J. Med. Chem.* **2006**, *49*, 1356−1363.

(50) Carroll, J.; Jonsson, E. N.; Ebel, R.; Hartman, M. S.; Holman, T. R.; Crews, P. Probing Sponge-Derived Terpenoids for Human 15-Lipoxygenase Inhibitors. *J. Org. Chem.* **2001**, *66*, 6847−6851.

(51) Whitman, S.; Gezginci, M.; Timmermann, B. N.; Holman, T. R. Structure-Activity Relationship Studies of Nordihydroguaiaretic Acid Inhibitors toward Soybean, 12-Human, and 15-Human Lipoxygenase. *J. Med. Chem.* **2002**, *45*, 2659−2661.

(52) Amagata, T.; Whitman, S.; Johnson, T. A.; Stessman, C. C.; Loo, C. P.; Lobkovsky, E.; Clardy, J.; Crews, P.; Holman, T. R. Exploring Sponge-Derived Terpenoids for Their Potency and Selectivity against 12-Human, 15-Human, and 15-Soybean Lipoxygenases. *J. Nat. Prod.* **2003**, *66*, 230−235.

(53) Cichewicz, R. H.; Kenyon, V. A.; Whitman, S.; Morales, N. M.; Arguello, J. F.; Holman, T. R.; Crews, P. Redox Inactivation of Human 15-Lipoxygenase by Marine-Derived Meroditerpenes and Synthetic

Chromanes: Archetypes for a Unique Class of Selective and Recyclable Inhibitors. *J. Am. Chem. Soc.* **2004**, *126*, 14910−14920.

(54) Vasquez-Martinez, Y.; Ohri, R. V.; Kenyon, V.; Holman, T. R.; Sepulveda-Boza, S. Structure-Activity Relationship Studies of Flavonoids as Potent Inhibitors of Human Platelet 12-Hlo, Reticulocyte 15-Hlo-1, and Prostate Epithelial 15-Hlo-2. *Bioorg. Med. Chem.* **2007**, *15*, 7408−7425.

(55) Deschamps, J. D.; Kenyon, V. A.; Holman, T. R. Baicalein Is a Potent in Vitro Inhibitor against Both Reticulocyte 15-Human and Platelet 12-Human Lipoxygenases. *Bioorg. Med. Chem.* **2006**, *14*, 4295−4301.

(56) Rai, G.; Kenyon, V.; Jadhav, A.; Schultz, L.; Armstrong, M.; Jameson, J. B.; Hoobler, E.; Leister, W.; Simeonov, A.; Holman, T. R.; Maloney, D. J. Discovery of Potent and Selective Inhibitors of Human Reticulocyte 15-Lipoxygenase-1. *J. Med. Chem.* **2010**, *53*, 7392−7404.

(57) Ngu, K.; Weinstein, D. S.; Liu, W.; Langevine, C.; Combs, D. W.; Zhuang, S.; Chen, X.; Madsen, C. S.; Harper, T. W.; Ahmad, S.; Robl, J. A. Pyrazole-Based Sulfonamide and Sulfamides as Potent Inhibitors of Mammalian 15-Lipoxygenase. *Bioorg. Med. Chem. Lett.* **2011**, *21*, 4141−4145.

(58) Weinstein, D. S.; Liu, W.; Gu, Z.; Langevine, C.; Ngu, K.; Fadnis, L.; Combs, D. W.; Sitkoff, D.; Ahmad, S.; Zhuang, S.; Chen, X.; Wang, F. L.; Loughney, D. A.; Atwal, K. S.; Zahler, R.; Macor, J. E.; Madsen, C. S.; Murugesan, N. Tryptamine and Homotryptamine-Based Sulfonamides as Potent and Selective Inhibitors of 15-Lipoxygenase. *Bioorg. Med. Chem. Lett.* **2005**, *15*, 1435−1440.

(59) Weinstein, D. S.; Liu, W.; Ngu, K.; Langevine, C.; Combs, D. W.; Zhuang, S.; Chen, C.; Madsen, C. S.; Harper, T. W.; Robl, J. A. Discovery of Selective Imidazole-Based Inhibitors of Mammalian 15-Lipoxygenase: Highly Potent against Human Enzyme within a Cellular Environment. *Bioorg. Med. Chem. Lett.* **2007**, *17*, 5115−5120.

(60) Malterud, K. E.; Rydland, K. M. Inhibitors of 15-Lipoxygenase from Orange Peel. *J. Agric. Food Chem.* **2000**, *48*, 5576−5580.

(61) Sailer, E. R.; Schweizer, S.; Boden, S. E.; Ammon, H. P. T.; Safayhi, H. Characterization of an Acetyl-11-keto-B-boswellic Acid and Arachidonate-Binding Regulatory Site of 5-Lipoxygenase Using Phoroaffinity Labeling. *Eur. J. Biochem.* **1998**, *256*, 364−368.

(62) Sendobry, S. M.; Cornicelli, J. A.; Welch, K.; Bocan, T.; Tait, B.; Trivedi, B. K.; Colbry, N.; Dyer, R. D.; Feinmark, S. J.; Daugherty, A. Attenuation of Diet-Induced Atherosclerosis in Rabbits with a Highly Selective 15-Lipoxygenase Inhibitor Lacking Significant Antioxidant Properties. *Br. J. Pharmacol.* **1997**, *120*, 1199−1206.

(63) Diana, G. D.; Treasurywala, A. M.; Bailey, T. R.; Oglesby, R. C.; Pevear, D. C.; Dutko, F. J. A Model for Compounds Active against Human Rhinovirus-14 Based on X-ray Crystallography Data. *J. Med. Chem.* **1990**, *33*, 1306−1311.

(64) Xia, Q.; Ganem, B. Metal-Mediated Variants of the Passerini Reaction: A New Synthesis of 4-Cyanooxazoles. *Synthesis* **2002**, *14*, 1969−1972.

(65) Dewar, M. J. S.; Turchi, I. J. Cornforth Rearrangement. *J. Am. Chem. Soc.* **1974**, *96*, 6148−6152.

(66) Boros, E. E.; Johns, B. A.; Garvey, E. P.; Koble, C. S.; Miller, W. H. Synthesis and HIV-Integrase Strand Transfer Inhibition Activity of 7-Hydroxy[1,3]thiazolo[5,4-b]pyridin-5(4H)-ones. *Bioorg. Med. Chem. Lett.* **2006**, *16*, 5668−5672.

(67) Ratan, R. R.; Murphy, T. H.; Baraban, J. M. Oxidative Stress Induces Apoptosis in Embryonic Cortical Neurons. *J. Neurochem.* **1994**, *62*, 376−379.

(68) Ratan, R. R.; Ryu, H.; Lee, J.; Mwidau, A.; Neve, R. L. In Vitro Model of Oxidative Stress in Cortical Neurons. *Methods Enzymol.* **2002**, *352*, 183−190.

(69) Murphy, T. H.; Schnaar, R. L.; Coyle, J. T. Immature Cortical Neurons Are Uniquely Sensitive to Glutamate Toxicity by Inhibition of Cystine Uptake. *FASEB J.* **1990**, *4*, 1624−1633.

(70) van Leyen, K.; Siddiq, A.; Ratan, R. R.; Lo, E. H. Proteasome Inhibition Protects HT22 Neuronal Cells from Oxidative Glutamate Toxicity. *J. Neurochem.* **2005**, *92*, 824−830.

(71) Zhang, J. H.; Chung, T. D.; Oldenburg, K. R. A Simple Statistical Parameter for Use in Evaluation and Validation of High Throughput Screening Assays. *J. Biomol. Screening* **1999**, *4*, 67−73.

(72) Mogul, R.; Johansen, E.; Holman, T. R. Oleyl Sulfate Reveals Allosteric Inhibition of Soybean Lipoxygenase-1 and Human 15-Lipoxygenase. *Biochemistry* **2000**, *39*, 4801−4807.

(73) Wecksler, A. T.; Kenyon, V.; Deschamps, J. D.; Holman, T. R. Substrate Specificity Changes for Human Reticulocyte and Epithelial 15-Lipoxygenases Reveal Allosteric Product Regulation. *Biochemistry* **2008**, *47*, 7364−75.

(74) Karatas, H.; Erdener, S. E.; Gursoy-Ozdemir, Y.; Gurer, G.; Soylemezoglu, F.; Dunn, A. K.; Dalkara, T. Thrombotic Distal Middle Cerebral Artery Occlusion Produced by Topical FeCl(3) Application: A Novel Model Suitable for Intravital Microscopy and Thrombolysis Studies. *J. Cereb. Blood Flow Metab.* **2011**, *31*, 1452−1460.

(75) Ohri, R. V.; Radosevich, A. T.; Hrovat, K. J.; Musich, C.; Huang, D.; Holman, T. R.; Toste, F. D. A Re(V)-Catalyzed C-N Bond-Forming Route to Human Lipoxygenase Inhibitors. *Org. Lett.* **2005**, *7*, 2501−2504.

(76) Chen, X. S.; Brash, A. R.; Funk, C. D. Purification and Characterization of Recombinant Histidine-Tagged Human Platelet 12-Lipoxygenase Expressed in a Baculovirus/Insect Cell System. *Eur. J. Biochem.* **1993**, *214*, 845−852.

(77) Robinson, S. J.; Hoobler, E. K.; Riener, M.; Loveridge, S. T.; Tenney, K.; Valeriote, F. A.; Holman, T. R.; Crews, P. Using Enzyme Assays to Evaluate the Structure and Bioactivity of Sponge-Derived Meroterpenes. *J. Nat. Prod.* **2009**, *72*, 1857−1863.

(78) Hoobler, E. K.; Holz, C.; Holman, T. R. Pseudoperoxidase Investigations of Hydroperoxides and Inhibitors with Human Lipoxygenases. *Bioorg. Med. Chem.* **2013**, *21*, 3894−3899.

(79) Kenyon, V.; Rai, G.; Jadhav, A.; Schultz, L.; Armstrong, M.; Jameson, J. B., 2nd; Perry, S.; Joshi, N.; Bougie, J. M.; Leister, W.; Taylor-Fishwick, D. A.; Nadler, J. L.; Holinstat, M.; Simeonov, A.; Maloney, D. J.; Holman, T. R. Discovery of Potent and Selective Inhibitors of Human Platelet-Type 12- Lipoxygenase. *J. Med. Chem.* **2011**, *54*, 5485−5497.